

## Control of magnetoelastic coupling in Ni/Fe multilayers using He<sup>+</sup> ion irradiation

G. Masciocchi,<sup>1,2, a)</sup> J. W. van der Jagt,<sup>3,4</sup> M.-A. Syskaki,<sup>1,5</sup> A. Lamperti,<sup>6</sup> N. Wolff,<sup>7</sup> A. Lotnyk,<sup>8</sup> J. Langer,<sup>5</sup> L. Kienle,<sup>7</sup> G. Jakob,<sup>1</sup> B. Borie,<sup>3</sup> A. Kehlberger,<sup>2</sup> D. Ravelosona,<sup>3,9</sup> and M. Kläui<sup>1</sup>

<sup>1)</sup>*Institute of Physics, Johannes Gutenberg University Mainz, Staudingerweg 7, 55099 Mainz, Germany*

<sup>2)</sup>*Sensitec GmbH, Walter-Hallstein-Straße 24, 55130 Mainz, Germany*

<sup>3)</sup>*Spin-Ion Technologies, 10 boulevard Thomas Gobert, 91120 Palaiseau, France*

<sup>4)</sup>*Université Paris-Saclay, 3 rue Juliot Curie, 91190 Gif-sur-Yvette, France*

<sup>5)</sup>*Singulus Technologies AG, Hanauer Landstrasse 107, 63796 Kahl am Main, Germany*

<sup>6)</sup>*CNR-IMM, UoS Agrate Brianza, Via Olivetti 2, 20864 Agrate Brianza, Italy*

<sup>7)</sup>*Faculty of Engineering, Institute for Material Science, Synthesis and Real Structure, Kiel University, Kaiserstraße 2, 24143 Kiel, Germany*

<sup>8)</sup>*Leibniz Institute of Surface Engineering (IOM), Permoserstraße 15, Leipzig 04318, Germany*

<sup>9)</sup>*C2N, CNRS, Université Paris-Saclay, 10 boulevard Thomas Gobert, 91120 Palaiseau, France*

(Dated: 7 October 2022)

This study reports the effects of post-growth  $\text{He}^+$  irradiation on the magneto-elastic properties of a  $\text{Ni}/\text{Fe}$  multi-layered stack. The progressive intermixing caused by  $\text{He}^+$  irradiation at the interfaces of the multilayer allows us to tune the saturation magnetostriction value with increasing  $\text{He}^+$  fluences, and even to induce a reversal of the sign of the magnetostrictive effect. Additionally, the critical fluence at which the absolute value of the magnetostriction is dramatically reduced is identified. Therefore insensitivity to strain of the magnetic stack is nearly reached, as required for many applications. All the above mentioned effects are attributed to the combination of the negative saturation magnetostriction of sputtered Ni, Fe layers and the positive magnetostriction of the  $\text{Ni}_x\text{Fe}_{1-x}$  alloy at the intermixed interfaces, whose contribution is gradually increased with irradiation. Importantly the irradiation does not alter the layers polycrystalline structure, confirming that post-growth  $\text{He}^+$  ion irradiation is an excellent tool to tune the magneto-elastic properties of magnetic samples. A new class of spintronic devices can be envisioned with a material treatment able to arbitrarily change the magnetostriction with ion-induced "magnetic patterning".

---

<sup>a)</sup>Electronic mail: gmascioc@uni-mainz.de

The magnetoelastic properties of thin films are of major interest for technological use as well as for scientific investigations. The requirements for the magnetoelastic coefficient ( $\lambda_s$ ) strongly depend on the application. Magnetic sensors often need, for example, strain immunity<sup>1</sup>, i.e. zero magnetostriction, to reduce strain cross-sensitivity, while actuators require giant strain effects, achieved in materials such as  $TbFe_2$  (terfenol)<sup>2</sup>. One way to obtain the optimal value of the magnetostriction for a specific application, is to use the combination of two or more materials with different magnetic and magnetoelastic properties. Multilayer systems have been widely investigated exploiting the combination of different parameters  $\lambda_s$  to achieve a target value<sup>3-6</sup>. In these studies, atomic intermixing at the multilayer interfaces has been identified to severely influence the total magnetostriction and this interface magnetostriction has been exploited to engineer the total magnetoelastic coupling of the multilayer<sup>3,4</sup>. In ion-sputtered films, where interface mixing naturally occurs, Nagai et al.<sup>3</sup> were able to change the sign of the magnetostriction of a multilayer magnetic stack by changing the relative thickness of the layers. However, a clear limit to this obsolete approach is the lack of control of the inter-layer roughness and degree of intermixing. The latter is indeed fixed by the deposition conditions. This imposes limitations to the usability of this method, as the magnetostriction cannot be arbitrarily nor locally changed.

A widely used technique to modify magnetic properties<sup>7-9</sup> and induce mixing at interfaces<sup>10,11</sup> is ion irradiation. Specifically, the use of light ions such as  $He^+$  at energies in the range of 10 – 30 keV induces short range atomic displacements without generation of surface defects in the material, which instead is more prevailing for heavy atoms<sup>12</sup> such as  $Ar^+$  or  $Ga^+$ . If compared to alternative techniques to promote atomic diffusion, e.g. annealing, the use of ion irradiation confines the intermixing to the magnetic layer boundaries and avoids mixing with the nonmagnetic seed layers (for details see Fig. S1 of the supplementary materials). Additionally, annealing is a uniform process while the local nature of irradiation interaction can be applied to the magnetic patterning of multilayer film system. For these reasons, ion irradiation is an excellent candidate to obtain a desired value of the magnetostriction in a multilayer, by controlling the vertical extension of the intermixed part. Previous work<sup>13</sup> reported intermixing induced magnetostriction changes using heavy ions and high energies (700 MeV). However, the use of these type of atoms can be harmful for thin magnetic layers<sup>14</sup>, whose magnetic properties such as saturation magnetization or perpendicular magnetic anisotropy can be easily degraded. Moreover, the presence of cascade collisions in the material and long-range atomic displacements<sup>15</sup> makes the precise control of magnetic properties a difficult task.

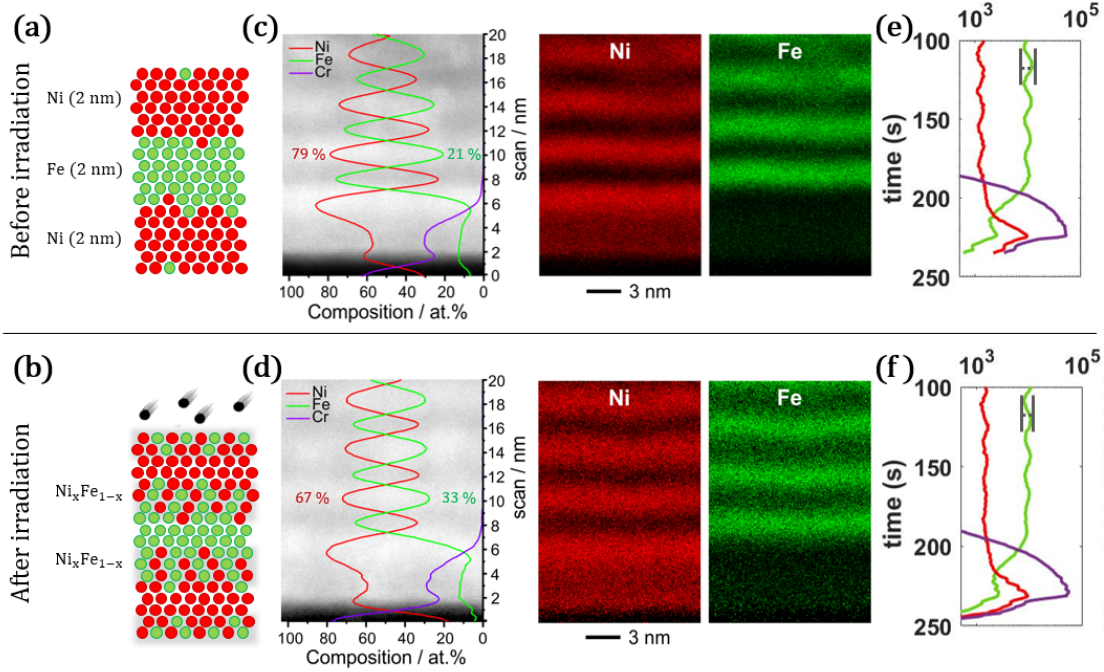


FIG. 1: (a) - (b) Sketch of the intermixing due to light ion irradiation on a multilayer stack. STEM HAADF micrograph and EDX elemental maps of the Fe/Ni multilayer system before (c) and after (d)  $1 \times 10^{16} \text{ cm}^{-2} \text{ He}^+$  ion irradiation measured across the first four repetitions on top of the NiFeCr seed layer. The HAADF micrograph is superimposed with a plot of the atomic composition quantified from the EDX measurements. (e) - (f) Depth distribution of the elements composing the multilayer structure obtained with ToF-SIMS in the as-deposited and irradiated samples respectively.

In this work, we study the effect of progressive intermixing at the interfaces of a *Ni/Fe* multilayer caused by light-ion irradiation at different fluences. We report that  $\text{He}^+$  ion irradiation can be used to tune locally the magnetoelastic properties of in-plane magnetized *Ni/Fe* multilayers, changing the saturation magnetostriction  $\lambda_s$  of the magnetic stack from negative to positive. Importantly, we confirm that the above mentioned method not only preserves the layers polycrystalline structure, but also improves the magnetic softness of the material, reducing the coercive field up to 70% and the anisotropy. The key advantages of the proposed method are the high repeatability of the process and the surface uniformity of the magnetic properties. Moreover this technology allows for ion-induced "magnetic patterning", with focused ions or performing the irradiation through a mask in a similar fashion to semiconductor doping<sup>11,16</sup>. Accordingly this technique is suitable to prepare channels for magnetic domain wall motion<sup>17,18</sup> and skyrmions<sup>19,20</sup> as it provides for the

creation of magnetoelastic coupling gradients.

The samples have been prepared by magnetron sputtering using a Singulus Rotaris system on a  $\text{SiO}_x/\text{Si}$  substrate. A multilayer of  $[\text{Ni}(2\text{ nm})/\text{Fe}(2\text{ nm})] \times 8$  is sputtered in the presence of a rotating magnetic field of  $5\text{ mT}$  on a  $\text{NiFeCr}$  ( $5\text{ nm}$ ) seed layer and capped with  $4\text{ nm}$  of  $\text{Ta}$ . After that, optical lithography and ion etching have been used to pattern arrays of circles ( $80\text{ }\mu\text{m}$  of diameter and  $3\text{ }\mu\text{m}$  of spacing) on the samples in order to probe the local film properties. Multiple copies of the samples have been irradiated at an energy of  $20\text{ keV}$  with different fluences of  $\text{He}^+$  ions from  $5 \times 10^{13}$  to  $1 \times 10^{16}\text{ cm}^{-2}$ . As reported elsewhere for similar irradiation conditions<sup>11</sup>, collision cascades are absent and the structural modifications are confined to the vicinity of the ion path in the metal.

At low fluences, it has been shown<sup>21</sup> that room temperature irradiation releases strain, whereas, at high fluences, one major structural effect of irradiation is intermixing, as schematically presented in Figs. 1 (a) and (b) and confirmed by Montecarlo (TRIM) simulations (Fig. S4 of the supplementary material). X-ray diffraction and scanning transmission electron microscopy (STEM) studies indicate in our sample a polycrystalline structure of (110)-textured layers of Fe and (111)-textured layers of Ni which is not significantly altered by the process of irradiation. In-depth investigation on the structural changes induced by  $\text{He}^+$  irradiation and annealing can be found in section S1 of the supplementary material, where atomic diffusion activated by thermal energy is compared with ion irradiation. According to TRIM simulations<sup>22</sup>, the majority (95%) of the ions reaches the substrate therefore a uniform intermixing in the vertical direction of the sample is expected, moreover, the effect of ion implantation in the multilayer is negligible.

To have a more quantitative estimation of the formation of the alloy for increasing ion fluences, a series of experiments to probe structural and chemical modifications occurring at the layer interfaces caused by ion irradiation were performed and are summarized in Fig. 1. Cross sections of Fe/Ni/NiFeCr on  $\text{SiO}_2/\text{Si}$  were prepared using the focused-ion-beam method (FIB). STEM electron energy-loss spectroscopy (EELS) was performed on a JEOL JEM-ARM200F “Neoarm” microscope operated at  $200\text{ kV}$  to determine the thickness of the prepared multilayers samples. High-angle annular darkfield scanning transmission electron microscopy (HAADF-STEM,  $80\text{-}200\text{ mrad}$ ) images were acquired and nanoscale chemical analysis via energy dispersive X-ray spectroscopy (EDX) was performed in STEM mode. A vertical EDX profile across the bottom layers of the multilayer stack is shown in Figs. 1 (c) and (d) together with corresponding EDX maps of the elemental distribution recorded on multilayers before and after  $\text{He}^+$  irradiation with  $1 \times 10^{16}$

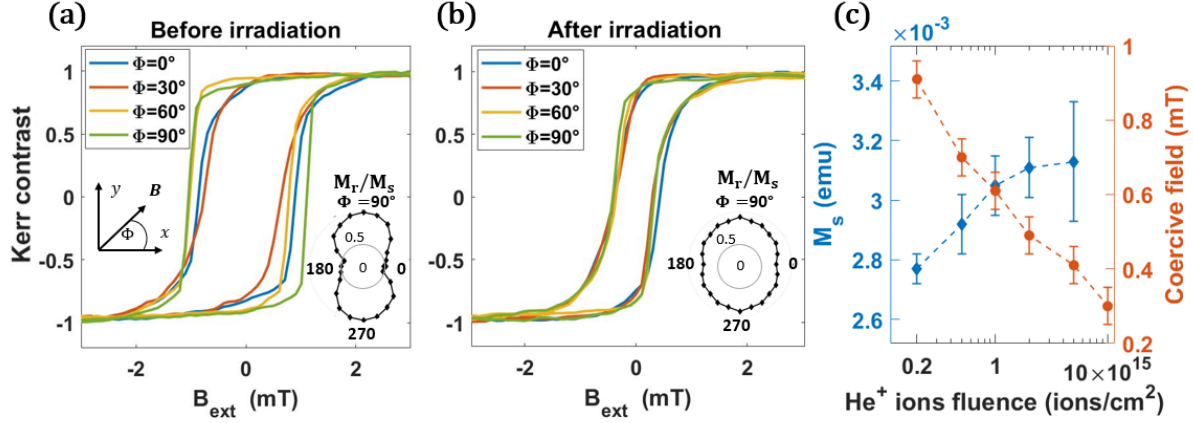


FIG. 2: (a) - (b) Hysteresis loops as a function of the in-plane magnetic field direction measured by Kerr microscopy, respectively, before and after ion irradiation with a fluence of  $1 \times 10^{16} \text{ cm}^{-2}$ . As inset, angular plot of the remanent magnetization  $M_r/M_s$  as a function of the magnetic field angle  $\Phi$ . (c) Saturation magnetic moment (light blue) and coercive field (orange) as a function of the fluence of  $\text{He}^+$  ions during irradiation measured with VSM.

$\text{cm}^{-2}$  fluence, respectively. After sputtering (Fig. 1 (c) ) the interfaces between the magnetic layers are well defined. The EDX profile of the relative atomic composition indicates 21(2)% of Fe in a Ni layer before the irradiation. After irradiation (Fig. 1 (d) ) the ratio of Fe atoms in a Ni layer increases to 33(4)%. This measured stoichiometric change in the layer composition is reflected in the displayed EDX elemental maps by the increased diffuse scattering of signal intensity across the layer interfaces after irradiation. This suggests the formation of an alloy of  $\text{Ni}_x\text{Fe}_{1-x}$  at the Ni/Fe interfaces when the different atoms are displaced under the effect of incoming  $\text{He}^+$  ions.

Figs. 1 (e) and (f) display the atomic depth distribution measured by Time-of-Flight Secondary Ion Mass Spectrometry (ToF-SIMS)<sup>23–27</sup>. The presence of Fe, Ni and Cr atoms in the multilayer is reported for samples as-deposited and irradiated with  $1 \times 10^{16} \text{ cm}^{-2}$  fluence, respectively. Observing Fig. 1 (e) the position of the periodic oscillations of Ni and Fe appear well defined and have the same periodicity. The peak position, minima of Ni at maxima of Fe, reflects the layer distribution. The atomic distribution after irradiation is shown in Fig. 1 (f). In this case, the amplitude of Ni and Fe oscillations is significantly attenuated with respect to the as-deposited case. This is again attributed to the intermixing of the atoms in the neighbouring magnetic layers, leading to the formation of  $\text{Ni}_x\text{Fe}_{1-x}$  alloy. More details about simulations and measurements to probe structural modifications can be found in section S1 of the supplementary materials.

The thin film magnetic properties have been measured with Kerr microscopy and Vibrating

Sample Magnetometry (VSM). Figs. 2 (a) and (b) show in-plane hysteresis loops before and after the ion irradiation, respectively. In Fig. 2 (a), the as-deposited sample presents different magnetization curves for different angular directions of the magnetic field, indicating the presence of uniaxial crystalline anisotropy  $K_u \simeq 100 \text{ J/m}^3$  as can be observed in the inset. The coercivity, measured along the easy axis of magnetization is  $0.95(5) \text{ mT}$ . The same magnetic measurements are reported in Fig. 2 (b) for the sample after  $\text{He}^+$  irradiation of  $1 \times 10^{16} \text{ cm}^{-2}$ . The magnetic in-plane anisotropy is now negligible, as the the different hysteresis loops overlap. The coercivity is reduced to  $0.25(5) \text{ mT}$ . The reduction in coercivity and anisotropy might be related to a possible increase in the concentration of nucleation sites after irradiation, which allow domain formation and switching of the magnetization at lower fields. As the  $H_c$  and the magnetic anisotropy are reduced, the magnetic softness of our multilayer is improved by this material treatment. Fig. 2 (c) reports systematic measurements of the magnetic properties of our  $[\text{Ni}(2 \text{ nm})/\text{Fe}(2 \text{ nm})] \times 8$  multilayer as a function of the  $\text{He}^+$  fluence during irradiation. With increasing  $\text{He}^+$  fluence the magnetic moment of the sample increases by about 15%, from  $2.8(1)$  to  $3.1(2) \times 10^{-3} \text{ emu}$ . As reported elsewhere<sup>28</sup>, this is an indication of increased level of intermixing of our magnetic layers (Ni and Fe).

In order to evaluate the potential of ion irradiation to finely tune the magnetoelastic properties of a magnetic multilayer, the effective magnetic anisotropy in our sample has been measured under the application of mechanical strain by three-point bending method as previously reported<sup>29</sup>. Here the substrate is bent to exert a uniaxial strain on the sample. Since the magnetization is coupled to the external strain via the expression of the anisotropy energy<sup>30</sup> one way to probe the effect of the strain is to observe changes in the hysteretic behavior before and after mechanical deformation. More details can be found in section S2 of the supplementary material. The expression of the magnetoelastic anisotropy depends on the saturation magnetostriction  $\lambda_s$  of the material according to<sup>31</sup>

$$K_{ME} = \frac{3}{2} \lambda_s Y \varepsilon, \quad (1)$$

where  $Y$  is the Young's modulus and  $\varepsilon$  is the uniaxial tensile strain. If the directions of the crystalline and magnetoelastic uniaxial anisotropy are such that  $K_u \perp K_{ME}$ , the strain dependent effective in-plane anisotropy  $K_{eff}$  measured in the system can be written as sum of two terms according to<sup>32</sup>

$$K_{eff} = K_u + K_{ME}. \quad (2)$$

As the sign of  $K_{ME}$  can be negative or positive, depending on the value of  $\lambda_s$ , the total magnetic anisotropy can, respectively, increase or decrease in the presence of strain. To quantify  $K_{eff}$  hysteresis loops are measured using Kerr microscopy, where the magnetic field and the tensile strain are applied along the fixed direction  $\Phi = 0^\circ$ . As the considered relatively thick magnetic system is dominated by shape anisotropy and thus in-plane magnetized, changes to interface anisotropy caused by ion irradiation can be neglected in our calculations.

The hysteresis loops measured along the direction of the applied strain  $\epsilon_{xx} = 0.06\%$  are reported in Fig. 3 (a) for samples irradiated with different fluences of ions. In response to the applied strain, the irradiated samples have a different magnetic anisotropy field. By comparison with the magnetization curve in the absence of strain (dashed line) two potential scenarios are identified. When a tensile strain increases the anisotropy field in the direction parallel to  $\epsilon_{xx}$ ,  $K_{ME}$  and  $\lambda_s$  are negative. Our sample exhibits negative magnetoelastic coupling in the as-deposited state. On the other hand, if the strain direction becomes an easy-axis of magnetization (reduced anisotropy field),  $K_{ME}$  and  $\lambda_s$  are positive. This behavior is reported for larger fluences in the same magnetic stack.

As the difference between magnetic loops before and after the application of strain is proportional to the magnetoelastic anisotropy, the saturation magnetostriction ( $\lambda_s$ ) of our magnetic multilayer can be estimated<sup>33–35</sup> using Eq. 1 and Eq. 2. Fig. 3 (b) shows the saturation magnetostriction as a function of the fluence of  $\text{He}^+$  ions. In agreement with the behavior of the magnetic loops, the value of magnetostriction of the as deposited  $\text{Ni}/\text{Fe}$  multilayer is  $-2.6(5) \times 10^{-6}$ .  $\text{He}^+$  fluences larger than  $5 \times 10^{14} \text{ cm}^{-2}$  gradually reduce the absolute value of magnetostriction that then increases through positive values. The change of sign of the magnetoelastic coupling occurs for fluences between  $1 \times 10^{15}$  and  $2 \times 10^{15} \text{ cm}^{-2}$ .

An additional confirmation of the magnetic behavior of the magnetic stack under strain is obtained by imaging domain formation using the magneto-optical Kerr effect (MOKE). A vector image of the in-plane magnetization is obtained by the sum of horizontal and vertical components of the magnetic contrast. The MOKE images shown in Figs. 3 (c) - (e) present how the preferred direction of magnetization changes before and after the application of 0.06% uniaxial strain in  $80 \mu\text{m}$  disk patterned samples. This particular shape has been chosen since it minimizes the in-plane shape anisotropy. The remanent magnetic domain pattern of the multilayer as-deposited



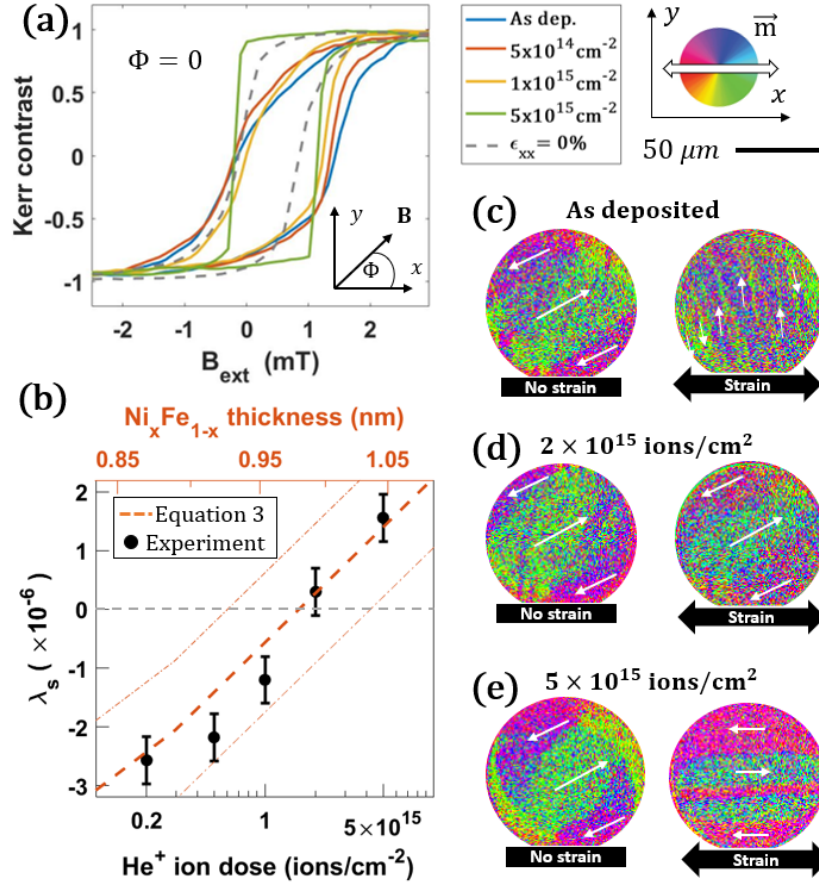


FIG. 3: (a) Hysteresis loops measured along the direction of the applied strain ( $\epsilon_{xx} = 0.06\%$ ) for different fluences of  $\text{He}^+$  ions (solid lines) are compared with the unstrained magnetic loop (dashed line). (b) Measured saturation magnetostriction  $\lambda_s$  (black dots) as a function of the ion fluence and calculated values using Eq. 3 (dashed line) as a function of the intermixed alloy thickness  $t_{\text{Ni}_x\text{Fe}_{1-x}}$ . A central value of  $\lambda_s^{\text{Ni}_x\text{Fe}_{1-x}} = 19 \times 10^{-6}$  with  $\pm 20\%$  variation is considered. Kerr microscope images of the remanent magnetic domain state respectively before (left) and after (right) the application of strain are compared for (c) as deposited case, (d) intermediate value of irradiation and (e) strong value of irradiation. White arrows represent the direction of the in-plane magnetization in the domains according to the color wheel.

is presented in Fig. 3 (c). Before the application of strain (left) the magnetization aligns to the crystalline anisotropy. After the application of strain magnetic domains orient along the  $y$  direction, perpendicular to the uniaxial strain  $\epsilon_{xx}$ . This is a clear experimental proof of the development of stress induced magnetic anisotropy  $K_{ME} \simeq -450 \text{ J/m}^3$  that overcomes the initial anisotropy direction.  $K_{ME}$  is perpendicular to the tensile strain direction due to the negative sign of the mag-

netostriction. The domain structure of the sample irradiated with a  $\text{He}^+$  dose of  $2 \times 10^{15} \text{ cm}^{-2}$  is displayed in Fig. 3 (d), where a value of magnetostriction close to zero is measured. In this case, the orientation of the magnetization is almost unchanged by the presence of strain, meaning that  $K_{ME}$  is negligible, compared to the crystalline anisotropy of the material  $K_u \simeq 100 \text{ J/m}^3$ . For higher values of fluences as reported in Fig. 3 (e), the effects of strain on the remanent magnetization state become again significant. This time the dominant magnetic anisotropy contribution in the system is  $K_{ME} \simeq 280 \text{ J/m}^3$  as the domains orient along the x direction, parallel to the applied strain  $\epsilon_{xx}$ . Thus, the magnetoelastic coupling of the stack has been altered using ion irradiation obtaining values of magnetostriction that range from negative to positive.

As previously reported<sup>4</sup>, the small value of magnetostriction in our (as-deposited) periodic system is caused by the balance among the negative magnetostriction of Ni ( $\lambda_s^{\text{Ni}} = -30 \times 10^{-6}$ ) and Fe ( $\lambda_s^{\text{Fe}} = -9 \times 10^{-6}$ ) and the strongly positive magnetostriction of  $\text{Ni}_x\text{Fe}_{1-x}$  alloy film ( $\lambda_s^{\text{NiFe}_{50}} = 19 \times 10^{-6}$ ) with a relative composition close to 50%<sup>36,37</sup>. As shown by STEM-EDX measurements, a more intermixed interface region of  $\text{Ni}_x\text{Fe}_{1-x}$  is formed at the boundary between Ni and Fe layers by  $\text{He}^+$  ion irradiation. Hence, the thickness of the positive magnetostrictive alloy increases proportionally to the fluence of the  $\text{He}^+$  ions during irradiation, as also confirmed by ToF-SIMS measurements. This gradually shifts the magnetostriction of the full stack to positive values. A common way to describe the effective magnetostriction in the presence of intermixing is<sup>3-6,38-40</sup>

$$\lambda_s = \frac{\lambda_s^{\text{Ni}} + \lambda_s^{\text{Fe}}}{2} + \left( 2\lambda_s^{\text{NiFe}_{1-x}} - \lambda_s^{\text{Ni}} - \lambda_s^{\text{Fe}} \right) \frac{t_{\text{NiFe}_{1-x}}}{t_p}, \quad (3)$$

where  $t_p = t_{\text{Ni}} + t_{\text{Fe}} = 4 \text{ nm}$  is the period thickness,  $t_{\text{NiFe}_{1-x}}$  describes the thickness of the alloy originated by the intermixing and  $\lambda_s^{\text{NiFe}_{1-x}}$  is the saturation magnetostriction of the intermixed alloy. With the appropriate magnetostriction values, Eq. 3 can be used to describe different material systems. The solution of Eq. 3 as a function of  $t_{\text{NiFe}_{1-x}}$  is shown in Fig. 3 (b) for the system investigated in this study. A central value of  $\lambda_s^{\text{NiFe}_{1-x}} = 19 \times 10^{-6}$  with  $\pm 20\%$  variation is considered. More details about the calculations are reported in section S1 of supplementary material. After deposition in similarly sputtered Ni/Fe multilayers<sup>3</sup>  $t_{\text{NiFe}_{1-x}}$  has been estimated to be around  $0.85 \text{ nm}$ , under the assumption  $t_{\text{Fe}}/t_p = 0.5$ . Using this value of  $t_{\text{NiFe}_{1-x}}$  Eq. 3 returns  $\lambda_s = -2.8(2) \times 10^{-6}$ , close to the measured value after deposition. Moreover, the amount of induced intermixing caused by  $\text{He}^+$  ions can be estimated using Eq. 3. The calculated  $t_{\text{NiFe}_{1-x}}$  is  $0.98(2) \text{ nm}$  at the magnetostriction compensation value ( $\lambda_s = 0$ ) and  $1.05(2) \text{ nm}$  for the highest

fluence, where the magnetostriction is positive due to the dominant effect of the alloy. This corresponds to 20% increase in the alloy thickness induced by  $\text{He}^+$  between  $0.2 \times 10^{15}$  and  $5 \times 10^{15} \text{ cm}^{-2}$ , in agreement with the information extracted from STEM-EDX and ToF-SIMS measurements.

In conclusion, this manuscript presents an experimental investigation in to the magnetoelastic properties of sputtered *Ni/Fe* multilayers after  $\text{He}^+$  ion irradiation. Using different experimental techniques for structural analysis, the presence of moderate roughness and alloying is observed after sputtering at the Ni/Fe interface. This can justify the small negative value of magnetostriction in the as-deposited state. In the same way, it was found that light ion irradiation promotes the intermixing of the sputtered layers at the interfaces proportional to the ion fluence. This process can explain the reported changes in the saturation magnetostriction of the magnetic stack. The increasing fluence of the irradiating ions progressively changes the saturation magnetostriction inducing a change in sign of the magnetoelastic coupling of the material, from negative to positive for high fluences. Remarkably, strain insensitivity on the magnetic properties of the proposed material can be obtained with ion fluences between  $1 \times 10^{15}$  and  $2 \times 10^{15} \text{ cm}^{-2}$ . Importantly, the polycrystalline structure of the layers is confirmed to be unchanged after the used irradiation conditions.

As a result, post growth  $\text{He}^+$  ion irradiation has been demonstrated to be an excellent tool that allows to fine-tune the magneto-elastic properties of multilayer magnetic samples and we expect this method to be applicable for several material combinations. Accordingly, this technique can be expected to be the next generation of material treatment offering the possibility to have local patterning of magnetostriction with high control and flexibility, allowing the realization of highly demanding and novel applications.

## SUPPLEMENTARY MATERIAL

See supplementary material for the complete characterization of the intermixing, the alloy composition and for details on the calculation of the magnetostriction.

## ACKNOWLEDGMENTS

The authors acknowledge Prof. J. McCord from Kiel University for fruitful discussions. This project has received funding from the European Union’s Horizon 2020 research and innovation program under the Marie Skłodowska-Curie grant agreement No 860060 “Magnetism and the effect of Electric Field” (MagnEFi), the Deutsche Forschungsgemeinschaft (DFG, German Research Foundation) - TRR 173 - 268565370 (project A01 and B02), the DFG funded collaborative research center (CRC)1261 / project A6 and the Austrian Research Promotion Agency (FFG). The authors acknowledge support by the chip production facilities of Sensitec GmbH (Mainz, DE), where part of this work was carried out and the Max-Planck Graduate Centre with Johannes Gutenberg University.

## AUTHOR DECLARATIONS

### Conflict of interest

The authors have no conflicts to disclose.

## DATA SHARING POLICY

The data that support the findings of this study are available from the corresponding author upon reasonable request.

## REFERENCES

- <sup>1</sup>S. Ota, A. Ando, and D. Chiba, “A flexible giant magnetoresistive device for sensing strain direction,” *Nature Electronics* **1**, 124–129 (2018).
- <sup>2</sup>H. García-Miquel, D. Barrera, R. Amat, G. Kurlyandskaya, and S. Sales, “Magnetic actuator based on giant magnetostrictive material Terfenol-D with strain and temperature monitoring using FBG optical sensor,” *Measurement* **80**, 201–206 (2016).
- <sup>3</sup>Y. Nagai, M. Senda, and T. Toshima, “Properties of ion-beam-sputtered Ni/Fe artificial lattice film,” *Journal of Applied Physics* **63**, 1136–1140 (1988).

- <sup>4</sup>M. Senda and Y. Nagai, “Magnetic properties of Fe/Co, Fe/CoFe, and (Fe/Co)/SiO<sub>2</sub> multilayer films,” *Journal of Applied Physics* **65**, 3151–3156 (1989).
- <sup>5</sup>S. Rengarajan, E. Yun, W. Kang, and R. Walser, “Effect of intermixing on the magnetic properties of Co<sub>50</sub>Fe<sub>50</sub>/Ni<sub>80</sub>Fe<sub>20</sub> multilayers,” *Journal of Applied Physics* **81**, 4761–4763 (1997).
- <sup>6</sup>S. Jen and C. Lin, “Magnetostriiction and Young’s modulus of [Fe<sub>15</sub>Ni<sub>85</sub>/Fe<sub>25</sub>Ni<sub>75</sub>] multilayers,” *Thin Solid Films* **471**, 218–223 (2005).
- <sup>7</sup>M. C. De Jong, M. J. Meijer, J. Lucassen, J. Van Liempt, H. J. Swagten, B. Koopmans, and R. Lavrijsen, “Local control of magnetic interface effects in chiral Ir/ Co/ Pt multilayers using Ga<sup>+</sup> ion irradiation,” *Physical Review B* **105**, 064429 (2022).
- <sup>8</sup>L. H. Diez, M. Voto, A. Casiraghi, M. Belmeguenai, Y. Roussigné, G. Durin, A. Lamperti, R. Mantovan, V. Sluka, V. Jeudy, *et al.*, “Enhancement of the Dzyaloshinskii-Moriya interaction and domain wall velocity through interface intermixing in Ta/CoFeB/MgO,” *Physical Review B* **99**, 054431 (2019).
- <sup>9</sup>L. Koch, F. Samad, M. Lenz, and O. Hellwig, “Manipulating the Energy Balance of Perpendicular-Anisotropy Synthetic Antiferromagnets by He<sup>+</sup>-Ion Irradiation,” *Physical Review Applied* **13**, 024029 (2020).
- <sup>10</sup>X. Zhao, B. Zhang, N. Vernier, X. Zhang, M. Sall, T. Xing, L. H. Diez, C. Hepburn, L. Wang, G. Durin, *et al.*, “Enhancing domain wall velocity through interface intermixing in W-CoFeB-MgO films with perpendicular anisotropy,” *Applied Physics Letters* **115**, 122404 (2019).
- <sup>11</sup>J. Fassbender, D. Ravelosona, and Y. Samson, “Tailoring magnetism by light-ion irradiation,” *Journal of Physics D: Applied Physics* **37**, R179 (2004).
- <sup>12</sup>B. Terris, L. Folks, D. Weller, J. Baglin, A. Kellock, H. Rothuizen, and P. Vettiger, “Ion-beam patterning of magnetic films using stencil masks,” *Applied Physics Letters* **75**, 403–405 (1999).
- <sup>13</sup>J. Juraszek, A. Grenier, J. Teillet, N. Tiercelin, F. Petit, J. B. Youssef, and M. Toulemonde, “Swift ion irradiation of magnetostrictive multilayers,” *Nuclear Instruments and Methods in Physics Research Section B: Beam Interactions with Materials and Atoms* **245**, 157–160 (2006).
- <sup>14</sup>W. F. Cureton, C. L. Tracy, and M. Lang, “Review of swift heavy ion irradiation effects in CeO<sub>2</sub>,” *Quantum Beam Science* **5**, 19 (2021).
- <sup>15</sup>T. Devolder, I. Barisic, S. Eimer, K. Garcia, J.-P. Adam, B. Ockert, and D. Ravelosona, “Irradiation-induced tailoring of the magnetism of CoFeB/MgO ultrathin films,” *Journal of Applied Physics* **113**, 203912 (2013).

- <sup>16</sup>T. Devolder, C. Chappert, Y. Chen, E. Cambril, H. Launois, H. Bernas, J. Ferre, and J. Jamet, “Patterning of planar magnetic nanostructures by ion irradiation,” *Journal of Vacuum Science & Technology B: Microelectronics and Nanometer Structures Processing, Measurement, and Phenomena* **17**, 3177–3181 (1999).
- <sup>17</sup>S. An, E. Baek, J.-A. Kim, K.-S. Lee, and C.-Y. You, “Improved spin-orbit torque induced magnetization switching efficiency by helium ion irradiation,” *Scientific reports* **12**, 1–10 (2022).
- <sup>18</sup>H. T. Nembach, E. Jué, K. Poetzger, J. Fassbender, T. J. Silva, and J. M. Shaw, “Tuning of the Dzyaloshinskii-Moriya interaction by  $\text{He}^+$  ion irradiation,” *Journal of Applied Physics* **131**, 143901 (2022).
- <sup>19</sup>L.-M. Kern, B. Pfau, V. Deinhart, M. Schneider, C. Klose, K. Gerlinger, S. Wittrock, D. Engel, I. Will, C. M. Gunther, *et al.*, “Deterministic Generation and Guided Motion of Magnetic Skyrmions by Focused  $\text{He}^+$ -Ion Irradiation,” *Nano Letters* (2022).
- <sup>20</sup>M. Fattouhi, F. García-Sánchez, R. Yanes, V. Raposo, E. Martínez, and L. Lopez-Diaz, “Electric Field Control of the Skyrmion Hall Effect in Piezoelectric-Magnetic Devices,” *Physical Review Applied* **16**, 044035 (2021).
- <sup>21</sup>T. Devolder, S. Pizzini, J. Vogel, H. Bernas, C. Chappert, V. Mathet, and M. Borowski, “X-ray absorption analysis of sputter-grown Co/Pt stackings before and after helium irradiation,” *The European Physical Journal B-Condensed Matter and Complex Systems* **22**, 193–201 (2001).
- <sup>22</sup>J. F. Ziegler, M. D. Ziegler, and J. P. Biersack, “SRIM—the stopping and range of ions in matter (2010),” *Nuclear Instruments and Methods in Physics Research Section B: Beam Interactions with Materials and Atoms* **268**, 1818–1823 (2010).
- <sup>23</sup>A. Benninghoven, F. Rudenauer, and H. W. Werner, “Secondary ion mass spectrometry: basic concepts, instrumental aspects, applications and trends,” (1987).
- <sup>24</sup>R. N. Sodhi, “Time-of-Flight Secondary Ion Mass Spectrometry (ToF-SIMS):—versatility in chemical and imaging surface analysis,” *Analyst* **129**, 483–487 (2004).
- <sup>25</sup>J. C. Vickerman and D. Briggs, *ToF-SIMS: materials analysis by mass spectrometry* (IM publications, 2013).
- <sup>26</sup>A. Lamperti, E. Cianci, O. Salicio, L. Lamagna, S. Spiga, and M. Fanciulli, “Thermal stability of high- $\kappa$  oxides on  $\text{SiO}_2/\text{Si}$  or  $\text{Si}_x\text{N}_y/\text{SiO}_2/\text{Si}$  for charge-trapping nonvolatile memories,” *Surface and interface analysis* **45**, 390–393 (2013).
- <sup>27</sup>R. L. Conte, E. Martinez, A. Hrabec, A. Lamperti, T. Schulz, L. Nasi, L. Lazzarini, R. Mantovan, F. Maccherozzi, S. Dhesi, *et al.*, “Role of B diffusion in the interfacial Dzyaloshinskii-Moriya

- interaction in  $Ta/Co_{20}Fe_{60}B_{20}/MgO$  nanowires,” *Physical Review B* **91**, 014433 (2015).
- <sup>28</sup>S. Srivastava, R. Kumar, A. Gupta, R. Patel, A. Majumdar, and D. Avasthi, “Swift heavy ion induced mixing in Fe/Ni multilayer,” *Nuclear Instruments and Methods in Physics Research Section B: Beam Interactions with Materials and Atoms* **243**, 304–312 (2006).
- <sup>29</sup>G. Masciocchi, M. Fattouhi, A. Kehlberger, L. Lopez-Diaz, M.-A. Syskaki, and M. Kläui, “Strain-controlled domain wall injection into nanowires for sensor applications,” *Journal of Applied Physics* **130**, 183903 (2021).
- <sup>30</sup>A. Bur, T. Wu, J. Hockel, C.-J. Hsu, H. K. Kim, T.-K. Chung, K. Wong, K. L. Wang, and G. P. Carman, “Strain-induced magnetization change in patterned ferromagnetic nickel nanostructures,” *Journal of Applied Physics* **109**, 123903 (2011).
- <sup>31</sup>S. Finizio, M. Foerster, M. Buzzi, B. Krüger, M. Jourdan, C. A. Vaz, J. Hockel, T. Miyawaki, A. Tkach, S. Valencia, *et al.*, “Magnetic anisotropy engineering in thin film Ni nanostructures by magnetoelastic coupling,” *Physical Review Applied* **1**, 021001 (2014).
- <sup>32</sup>N. Martin, J. McCord, A. Gerber, T. Strache, T. Gemming, I. Mönch, N. Farag, R. Schäfer, J. Fassbender, E. Quandt, *et al.*, “Local stress engineering of magnetic anisotropy in soft magnetic thin films,” *Applied Physics Letters* **94**, 062506 (2009).
- <sup>33</sup>G. Choe and B. Megdal, “High precision magnetostriction measurement employing the BH loopster bending method,” *IEEE Transactions on Magnetics* **35**, 3959–3961 (1999).
- <sup>34</sup>A. Raghunathan, J. E. Snyder, and D. Jiles, “Comparison of alternative techniques for characterizing magnetostriction and inverse magnetostriction in magnetic thin films,” *IEEE Transactions on Magnetics* **45**, 3269–3273 (2009).
- <sup>35</sup>C. Hill, W. Hendren, R. Bowman, P. McGeehin, M. Gubbins, and V. Venugopal, “Whole wafer magnetostriction metrology for magnetic films and multilayers,” *Measurement Science and Technology* **24**, 045601 (2013).
- <sup>36</sup>R. M. Bozorth, *Ferromagnetism* (1993).
- <sup>37</sup>B. D. Cullity and C. D. Graham, *Introduction to magnetic materials* (John Wiley & Sons, 2011) Chap. 8, pp. 243–257.
- <sup>38</sup>M. Hollingworth, M. Gibbs, and S. Murdoch, “Magnetostriction and surface roughness of ultrathin NiFe films deposited on  $SiO_2$ ,” *Journal of Applied Physics* **94**, 7235–7239 (2003).
- <sup>39</sup>C. Favieres, J. Vergara, and V. Madurga, “Interface effects on magnetostriction in pulsed laser deposited Co/Fe/Co cylindrical soft magnetic multilayers,” *Journal of Physics D: Applied Physics* **40**, 4101 (2007).

<sup>40</sup>S. Jen, T. Wu, C. Lin, and K. Chang, “Anisotropic magnetoresistance and magnetostriction of  $[\text{Fe}_{15}\text{Ni}_{85}/\text{Fe}_{25}\text{Ni}_{75}]$  and  $[\text{Co}_{35}\text{Ni}_{65}/\text{Fe}_{25}\text{Ni}_{75}]$  multilayers,” Solid State Communications **132**, 259–262 (2004).